Development and Long-Term In Vivo Evaluation of a Biodegradable Urethane-Doped Polyester Elastomer

Jagannath Dey, Richard T. Tran, Jinhui Shen, Liping Tang, Jian Yang*

A detailed report on the development of CUPE polymers synthesized using diols with 4, 6, 8, 10, or 12 methylene units is presented with the aim of elucidating the influence of the diol component on the physical properties of the resulting material and assessing their long-term biological performance in vivo. Increasing the diol length leads to lower crosslinking densities, higher hydrophobicities, higher tensile strengths and elasticities, and slower polymer degradation. The choice of diol does not affect the overall cell/tissue compatibility both in vitro and in vivo. The diol component is thus established as an important parameter in controlling the structure/property relationships of the polymers, thereby increasing the choice of biodegradable elastomers for tissue engineering applications.

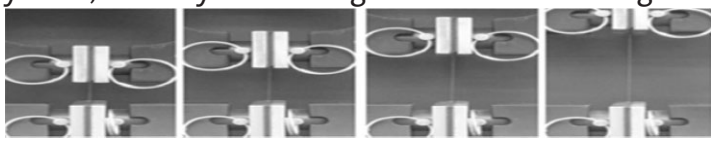

Introduction

The application of semicrystalline biodegradable polymers such as poly(L-lactic acid) (PLLA), poly(glycolic acid) (PGA), and their co-polymers has enabled significant progress in the engineering of hard tissues.[1–7] In contrast, there has been unsatisfactory progress in the engineering of soft tissues including blood vessels, heart valves, bladder, and cartilage primarily due to the limited available soft and elastic biomaterials. When materials are placed in a mechanically demanding environment, there is a potential to cause irritation the surrounding tissues if the implant material is not mechanically compliant.[8] Ideally, biomaterials should possess unique chemical, physical, and mechanical properties to mimic the extracellular matrix of the targeted tissue being regenerated.[9–12] In addition, the importance and effects of adequate mechanical conditioning on the expression of appropriate cellular phenotypes and extracellular matrix deposition have been well documented in numerous studies,[13–15] and it has also been reported that dissected soft tissues like nerves and blood vessels are nearly 30% shorter than their in situ length,[15] which further emphasizes the need for materials specifically designed to be elastic in nature for soft tissue replacement therapy.

In order to fulfill this need of materials suited for soft tissue engineering, researchers have developed numerous biodegradable and biocompatible elastomers over the past few years.[8,16–25] Poly(1,8-octanediol citrate) (POC) is one such biodegradable elastomer,[19,20] which has demonstrated excellent cell/tissue-compatibility and hemocompatibility.[26] Although biphasic tubular scaffolds fabricated from POC are attractive for potential use as small diameter vascular grafts due to their elasticity and hemocompatibility,[27] poor load bearing capabilities, and inadequate suture retention strengths limit the utility of POC.

To overcome the limitations of POC, we have recently reported on the synthesis and characterization of cross-

J. Dey, R. T. Tran, J. Shen, L. Tang, J. Yang
Department of Bioengineering, The University of Texas at Arlington, Arlington, TX 76019, USA
E-mail: jianyang@uta.edu

DOI: 10.1002/mame.201100074

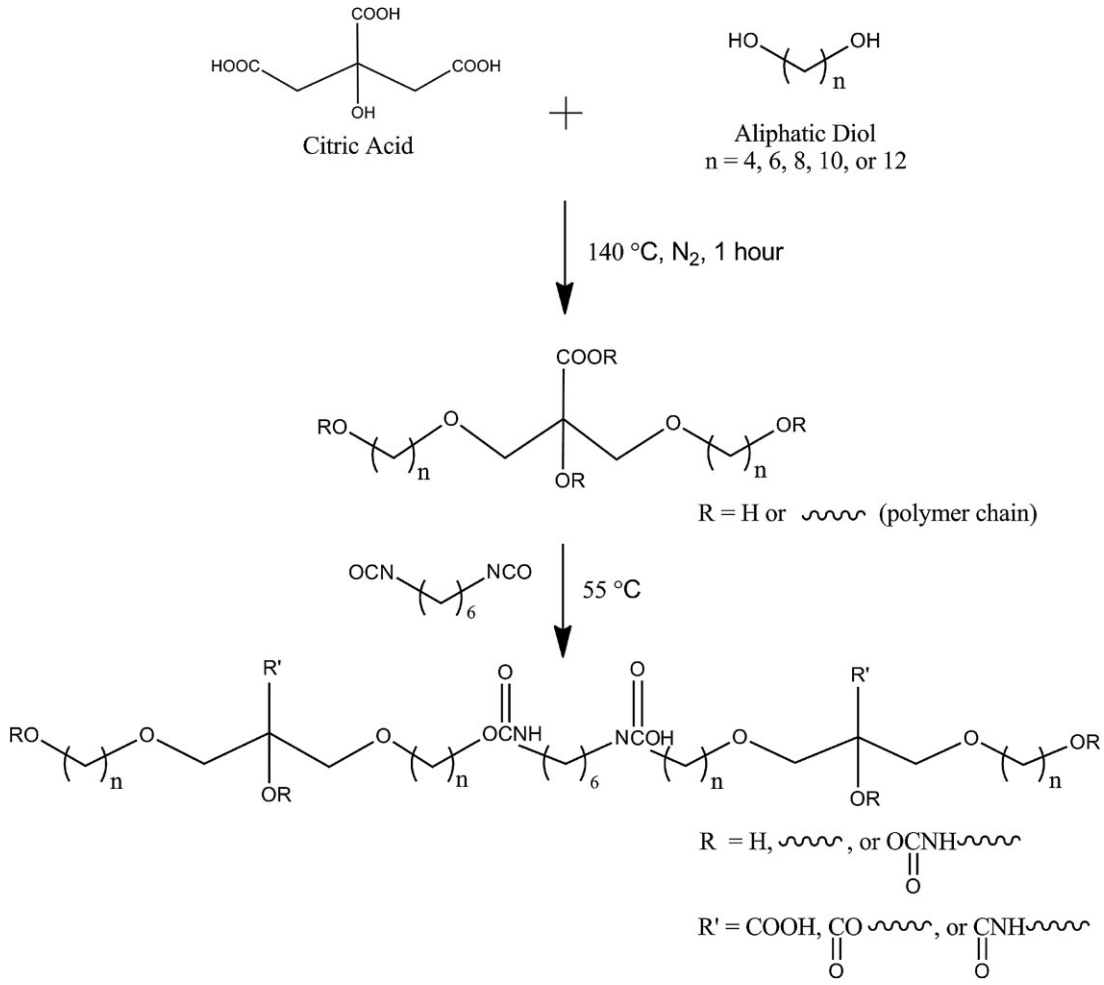

Figure 1. Representative CUPE synthesis schematic. The monomers citric acid and various aliphatic diols (4, 6, 8, 10, or 12 methylene units in length) underwent condensation polymerization to produce hydroxyl group capped pre-poly(diol citrates). Next, HDI was used to extend the pre-poly(diol citrates) to produce pre-CUPE. Pre-CUPE can be post-polymerized to obtain a crosslinked polyester network.

linked urethane-doped polyester (CUPE) networks, a novel biodegradable and biocompatible elastomer with excellent mechanical properties.[28] The superior mechanical strength of CUPE motivated the development tubular scaffolds, and further evaluation of the graft hemocompatibility.[29] Our earlier work on CUPE focused on a single polyester soft segment composition and examined the material's structure-property relationship as a function of the ratio of polyester to diisocyanate used in the synthesis.[28] In this current work, we have focused on investigating the effect of soft segment polymer composition on the resulting material and biological properties while keeping the ratio of polyester to diisocyanate constant. This study provides further evidence that CUPE is a highly flexible material whose properties can be controlled, and accurately matched to the target application by varying numerous reaction parameters.

Experimental Section

CUPE Synthesis

All chemicals, cell culture medium, and supplements were purchased from Sigma-Aldrich (St. Louis, MO), except where mentioned otherwise and used as received. The different CUPE polymers were synthesized via a three-step procedure reported previously (Figure 1).[28] Step 1 involves the polycondensation reaction of citric acid with different C4–C12 aliphatic diols: 1,4-butanediol (≥99%), 1,6-hexanediol (99%), 1,8-octanediol (98%), 1,10-decanediol (98%), or 1,12-dodecanediol (99%). Step 2 involves the introduction of urethane linkages to form the final CUPE prepolymer, and step 3 involves a post-polymerization step for final thermal crosslinking. Briefly, citric acid and various diols were bulk polymerized in a three-neck flask equipped with an inlet and outlet adapter, at 160–165 °C. A monomer ratio of 1:1.1 (acid to diol) was used for the all synthesis procedures. The temperature was reduced to 140 °C when the monomer mixture had melted, and the reaction

was allowed to continue for 1 h to obtain the soft segment pre-polymer. The resulting polymer was purified by drop-wise precipitation in de-ionized (DI) water under constant stirring. The purified pre-polymer precipitate was carefully collected from the aqueous phase and lyophilized for 48 h to remove traces of water. In step 2, the purified pre-polymer was dissolved in 1,4-dioxane to form a 3.0% solution (w/w), and the polymer solution was reacted with 1,6-hexamethylene diisocyanate (HDI) under constant stirring with stannous octoate as catalyst (0.1 wt%). The reaction was carried out at 55 °C, and reaction completion was indicated by the absence of a diisocyanate peak in the Fourier-transform infrared (FT-IR) spectrum of the reaction mixture at 2 267 cm^{-1}. In step 3, the pre-CUPE synthesized in step 2 was cast in Teflon molds, air dried to remove all solvent, and then cured in an oven maintained at 80 °C for time periods ranging from 1 to 4 d, to obtain the final crosslinked urethane-doped polyester.

The different crosslinked urethane-doped polyesters obtained were designated as CUPEX, where X denotes the number of carbon atoms in the diol used as the monomer for the reaction with citric acid. For example, CUPE10 indicates that 1,10-decanediol was the monomer used in the reaction. For all the different polymers obtained, the soft segment pre-polymer/diisocyanate ratio of 1:1.2 was maintained.

Polymer Characterization

A Nicolet 6700 FT-IR spectrometer (Thermo Fisher Scientific) was used to obtain FT-IR spectra of the different polymers synthesized. Briefly, a dilute solution (3.0 wt% of the CUPE pre-polymer dissolved in 1,4-dioxane was cast onto a clean potassium bromide (KBr) crystal, and allowed to dry in vacuum for 6 h prior to spectrum acquisition.

The glass transition temperature (T_g) of the different CUPE polymers synthesized was determined by differential scanning calorimetry (DSC) on a DSC2010 calorimeter (TA Instruments, New Castle, DE). The different polymer samples were subjected to two heating cycles. In the first cycle, the polymers were scanned to 150 °C, under nitrogen atmosphere with a step size of 10 °C · min^{-1} and then cooled rapidly to –60 °C at a cooling rate of –40 °C · min^{-1}. The second cycle comprised of heating the sample to 230 °C with a step size of 10 °C · min^{-1}. All readings were collected during the second heating scan. The T_g value was determined from the middle of any step changes in the heat capacity from the second scan. All mechanical testing was conducted on a MTS Insight 2 mechanical tester equipped with a 500 N load cell (MTS, Eden Prairie, MN). Mechanical testing was carried out to determine the effect of the different diols and different polymerization conditions on CUPE tensile properties. All films were cut into dog bone shape as per ASTM D412a standard ($25 \times 6 \times 1.5\ mm^3$). The samples were stretched at a deflection rate of 500 mm · min^{-1} until break. The initial modulus was derived from the gradient of the curve at 10% elongation in the stress/strain curve. A minimum sample size of $N = 5$ was maintained for all the films tested. A density measurement kit (Mettler Toledo, Columbus, OH) was used to determine the density of the different CUPE polymers synthesized. The auxiliary fluid used in the density measurement experiments was DI water. In order to determine the molecular weight between crosslinks and the crosslink density, the theory of rubber elasticity was used (Equation 1):[18–20,24]

$$\eta = \frac{E_0}{3RT} = \frac{\rho}{M_c} \quad (1)$$

where η is the number of moles of active network chains per unit volume, E_0 the initial modulus of the polymer, R the universal gas constant, T the absolute temperature, ρ the density of the polymer, and M_c is the relative molar mass between crosslinks. Contact angle measurements were made on the different CUPE thin films using the sessile drop method. A KSV101 optical contact angle and surface tension meter (KSV Instruments Inc, Helsinki, Finland) was used for obtaining the contact angle values. Thin films of the different CUPE pre-polymers were made by smearing 1 mL of a dilute polymer solution in 1,4-dioxane (3.0 wt% on a clean glass slide. All readings were collected within 10 s after drop elution. A minimum of 10 readings was collected from different regions of the different thin films from each sample.

In Vitro Degradation

An accelerated in vitro degradation study of the different CUPE polymers was carried out in 0.01 M sodium hydroxide (NaOH) solutions. Briefly, the polymer films were cut into 7 mm discs using a cork borer and the initial weights of these discs was recorded. The discs were transferred to clean test tubes containing 10 mL of 0.01 M NaOH and incubated at 37 °C for pre-determined time intervals of 3, 6, 9, and 12 h. A minimum of eight specimens per time point was present for each polymer being tested. At each time interval, first the NaOH was aspirated out of the test tube and the polymer samples were washed thoroughly with DI water twice to remove any traces of NaOH. The polymer samples were then lyophilized for 72 h to remove traces of water and weighed to obtain the final degraded weight corresponding to that time interval. The initial weight of the specimen and the degraded weight at a particular time interval were used to determine the rate of degradation of the polymer corresponding to that time interval using Equation 2,

$$\text{mass loss}(\%) = \frac{W_0 - W_t}{W_0} \times 100 \quad (2)$$

where W_0 is the initial weight of polymer disc and W_t is the final weight of the degrading polymer disc. A long-term degradation study was also conducted as per the aforementioned method using PBS as the degrading agent and CUPE8 as the representative polymer. The degradation of the polymer discs was monitored over a total period of 8 months.

In Vitro Cell Culture

The biocompatibility of the different CUPE polymers was evaluated by seeding the polymer films with two different cell lines and observing the morphology and proliferation of the cultured cells after 3 d post-seeding. Human aortic smooth muscle cells (HASMCs) and the NIH 3T3 fibroblasts were selected as the model cells lines for this assessment. Briefly, the polymer samples were cut into 10 mm diameter discs using a cork borer. These discs were sterilized by a

two-step process comprising of ultraviolet (UV) light treatment for 1 h followed by immersion in 70% ethanol for 30 min. The sterilized discs were washed thoroughly with sterile PBS to remove any traces of alcohol and then allowed to dry completely prior to cell seeding. Cells were cultured in 75 cm^2 culture flasks with Dulbecco's modified Eagle's medium (DMEM) supplemented with 10% fetal bovine serum. For seeding, the cells were trypsinized, centrifuged, and re-suspended in fresh complete culture medium. The volume of culture medium used to re-suspend the cell pellet was adjusted to obtain a seeding density of 3×10^5 cells $\cdot$ mL^{-1}. 200 μL of the cell suspension was evenly spread over the surface of each of the CUPE films being tested. After 1 h of incubation at 37 °C, 5 mL of complete culture medium was added to each of the Petri dishes containing the cell seeded films. The cells were cultured on the films for 3 d during which the media was changed daily.

At the end of the culture point, the cells on the polymer discs were fixed by addition of 5 mL of 2.5% (w/v) solution of gluteraldehyde in phosphate-buffered saline (PBS). All samples were kept in the fixating medium for at least 2 h. After fixation, the cells were sequentially dehydrated in a graded series of ethanol (50, 75, 90, and 100%) and lyophilized to remove any minute traces of water. The dehydrated cell seeded polymer discs were mounted on stubs, sputter coated with silver for 2 min, and observed under a Hitachi S300N (Hitachi Corp, Tokyo, Japan) scanning electron microscope (SEM). Different images of cellular morphology were captured at different magnifications to gauge the pattern of cellular growth and proliferation on the polymer surfaces.

Foreign Body Response

CUPE8 was used as the representative polymer to study the extent of foreign body response incited by the presence of the polymer for a medium term implantation period of 8 weeks and a long-term implantation period of 6 months. CUPE8 scaffolds and PLLA control scaffolds were prepared by salt leaching with a salt size of 150–250 μm. The scaffolds were cut into discs (10 mm × 1 mm, diameter × thickness) using a cork borer and implanted subcutaneously in the back of healthy, female Sprague Dawley (SD) rats (Harlan Sprague Dawley, Inc., Indianapolis, IN). Animals were cared for in compliance with regulations of the animal care and use committee of the University of Texas at Arlington. Prior to implantation, the discs were sterilized by treatment with 75% ethanol for 1 h followed by 1 h of UV light treatment. A total of eight rats were used for this study; four rats each for each time point of 8 weeks and 6 months. The rats were anesthetized using an isofluorane/oxygen mixture and the test samples were implanted in the upper back by blunt dissection.

At the end of each time period the rats tagged for that time period were sacrificed by CO_2 asphyxiation. The implant and the surrounding tissue was collected and frozen in OCT embedding media (Polysciences Inc., Warrington, PA), at −80 °C for further histological analysis. The tissue blocks were sectioned into 10 μm sections using a cryostat and stained with hematoxylin and eosin (H&E) to examine the tissue responses. Stained section images were acquired at 10× magnifications using a Leica DMLP microscope fitted with a Nikon E500 camera (Nikon Corp., Japan). A minimum of three images was obtained from each section for analysis, and three sections were examined per animal sacrificed. ImageJ software was used to determine the fibrous capsule thickness in each of the analyses performed. In order to determine an average fibrous response, at least 25 readings of capsule thickness were obtained from different parts of the section images obtained and averaged.

Statistical Analysis

All data obtained are presented as the mean ± standard deviation. The statistical significance between independent data sets was calculated using Student's two-tail t-test. A value $p < 0.05$ was used as a measure of significant difference.

Results and Discussion

Although elastomeric biomaterial development has been largely driven by the prerequisites of most soft tissues, elastic tissues vary greatly and cover a wide range of mechanical properties. For example, the mechanical properties of bladder tissue[30] vary greatly when compared to that of aortic tissue[31] or skin.[32] It has been well established that for successful tissue engineering one of the main requirements that need to be fulfilled is a similarity between the properties of the extracellular matrix of the target tissue and the replacement scaffold.[23,33–36] Being able to control the properties of a polymer through multiple modalities is especially important to improve the utility of a bio-polymer for diverse soft tissue engineering applications.[37]

In our previous work,[28] we successfully synthesized and characterized the physical and biological properties of crosslinked urethane-doped polyesters. From the results obtained, we were able to establish CUPE as a biodegradable, biocompatible, and strong yet soft elastomer. Although we concentrated primarily on the effects of different molar ratios of isocyanate to pre-polymer, we briefly demonstrated that the polymer properties could be manipulated by varying the diol component as well. The focus on controlling the material performance through various diols motivated us to explore the development of a family of such elastomers, whose diols varied in their methylene content.

FT-IR spectra obtained for all the synthesized polymers are depicted in Figure 2. The absence of an isocyanate peak at 2 267 cm^{-1} was characteristic of all the spectra obtained, which indicated that the synthesis of the different CUPE polymers consumed all the diisocyanate in the reaction process. The peaks centered at 1 733 cm^{-1} were assigned to carbonyl groups of the free carboxylic acid functional groups on the citric acid backbone and carbonyl groups of the ester bonds in the polymer backbone. Peaks between 2 931 and 2 919 cm^{-1} were assigned to the methylene units in the polymer backbone.[19,38] FT-IR also confirmed the incorporation of the isocyanate in the polymer backbone by urethane bond formation. All the CUPE polymers had sharp

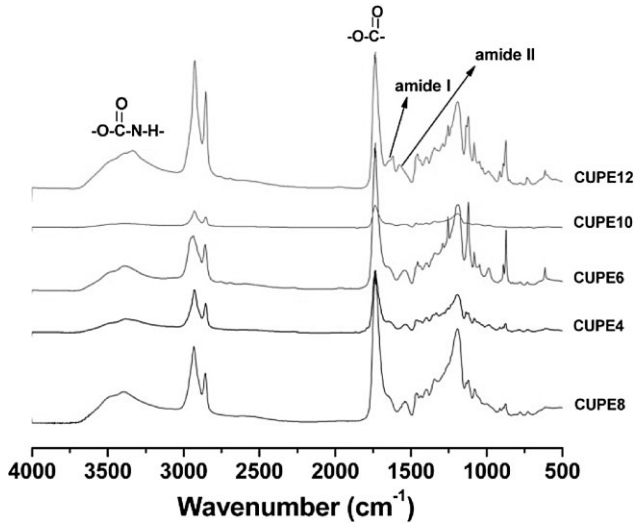

Figure 2. FT-IR spectra of the different crosslinked urethane-doped polyester pre-polymers synthesized with different diols. The pre-polymers include pre-CUPE4, pre-CUPE6, pre-CUPE8, pre-CUPE10, and pre-CUPE12.

peaks at 1 670 and 1 560 cm^{-1} which were attributed to amide I and amide II vibrations, respectively. A narrow shoulder peak at 3 350 cm^{-1} also suggests the presence of urethane linkages in the polymer chains.[39] Figure 3 depicts the glass transition temperature of the different CUPE polymers, as determined by DSC. No obvious hard segment transitions were observed in the DSC thermograms indicating a low degree of microphase separation in all the CUPE polymers examined.[40–42] Furthermore, all thermograms lacked any crystallization and melting peaks, indicating the absence of hard segment crystallization.[43] The glass transition temperature of the polymers varied as

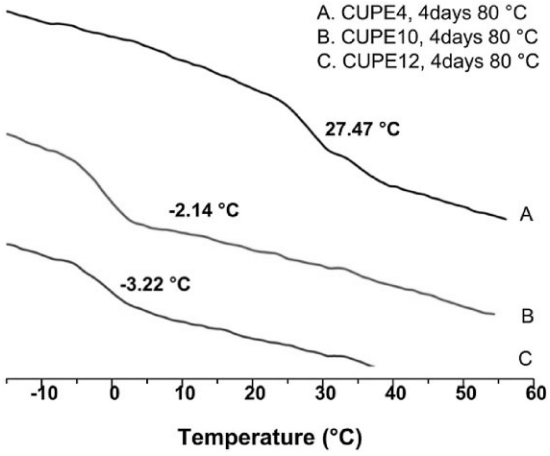

Figure 3. Effect of different diols on the DSC thermograms of the CUPE polymers. All samples tested were post-polymerized for 4 d at 80 °C prior to analysis. A two-step heating cycle was used to generate DSC thermograms for the different polymers.

an inverse function of the length of the diol component. CUPE12, which had the longest diol chain, had the lowest glass transition temperature ($T_g = -3.22$ °C), whereas, CUPE4, which had the smallest diol component, demonstrated a higher value of T_g (27.47 °C). CUPE8 which had a T_g value of 3.06 °C[28] also supports this trend. This increase in glass transition temperature with decreasing diol length may be explained by the segmented architecture of urethanes, wherein, strong hydrogen bonding between the polymer chains may function as physical crosslinks.[44] Increasing the length of the diol may serve to reduce the crosslink density by increasing the separation between the urethane groups in the polymer backbone, thus increasing the polymer chain mobility and subsequently lowering T_g. A decrease in the molecular weight of the soft segment would also promote an increase in the hard segment effect on the chain mobility as a result of phase mixing,[45] thus increasing the glass transition temperature of the CUPEs synthesized with smaller diols.

Assuming the different polymers recovered completely after deformation, the effect of diol length on the crosslink density of the crosslinked polyester network was further examined using the theory of rubber elasticity, which has been used in previous studies to evaluate other biodegradable polyester elastomers.[18–20,24] Data represented in Table 1 indicate that formulations with increasing diol length did indeed reduce the ester bond crosslink density allowed for by the citric acid component of the CUPE polymer. Under similar post-polymerization conditions (2 d at 80 °C) CUPE6 had the highest crosslink density of all the polymers evaluated ($\eta = 1\ 142.12 \pm 120.79$ mol $\cdot$ m^{-3}) while CUPE10 had the lowest crosslink density ($\eta = 783.07 \pm 167.52$ mol $\cdot$ m^{-3}). Increasing the post-polymerization duration to 4 d, also led to an increase in crosslink density due to the formation of more inter-chain ester bond crosslinking (CUPE10_4D $\eta = 978.31 \pm 157.26$ mol $\cdot$ m^{-3}). As a result of the growing length of methylene units in the polymer backbone with the incorporation of longer diols and subsequent increase in the molecular weight between crosslinks, the specific density of the different CUPE polymers decreased with increasing diol size (Table 1).[19]

All the CUPE polymers displayed break elongations exceeding 100% and elastomeric properties: full recovery of the sample dimensions after removal of applied stress. Increasing the length of the diol resulted in stronger polymers (Figure 4A). Under similar polymerization conditions of 2 d in an oven maintained at 80 °C, CUPE10 had the highest peak stress (38.36 ± 1.69 MPa) and CUPE6 was the weakest polymer (9.56 ± 2.00 MPa). This may be attributed to an increase in the molecular weight of the polymer due to the incorporation of higher molecular weight diols. The initial Young's modulus of the different polymers varied from 6.02 ± 1.07 to 8.00 ± 1.22 MPa, with CUPE6 being the

Table 1. Physical properties of the CUPE polymers.

Sample	Density [g · cm^{-3}]	Young's modulus [MPa]	Tensile strength [MPa]	N [mol · m^{-3}]	M_c [g · mol^{-1}]
CUPE6_2D	1.30 ± 0.05	8.00 ± 1.22	9.56 ± 2.00	1144.12 ± 120.79	1148.21 ± 140.97
CUPE8_2D	1.24 ± 0.01	7.02 ± 0.85	17.38 ± 2.34	951.40 ± 123.59	1320.47 ± 187.36
CUPE10_2D	1.15 ± 0.02	6.02 ± 1.07	24.19 ± 2.04	783.07 ± 167.52	1522.97 ± 351.14
CUPE10_4D	1.17 ± 0.02	7.22 ± 0.90	38.36 ± 1.69	978.31 ± 157.26	1130.972 ± 145.74

most stiff (Figure 4B), which could be attributed to the higher crosslink density in CUPE6, thereby, necessitating higher initial stress to cause deformation.[46,47] The higher crosslink density of polymers with lower number of methylene units in the diol also results in the polymers being more brittle, as can be seen from the increase in the final strain with increasing diol size (Figure 4C). In addition to diol concentration, increasing polymerization conditions resulted in stronger, stiffer, and more brittle polymers, which corresponds to our earlier results.[28] In order to assess the material's elastomeric properties in detail, hysteresis cycle was performed at room temperature. As a typical example, hysteresis cycle of CUPE8 films after the 10th elongation is shown in Figure 4D: 50% elongation and back at room temperature. CUPE8 samples showed excellent recovery with no loss of energy, which could be attributed to the strong intermolecular cohesive energy between the crosslinked polyester network components.

The influence of the monomers on the surface properties of the CUPE polymers is summarized in Figure 5. As expected, using a more hydrophobic diol in the synthesis of CUPEs resulted in more hydrophobic polymers. CUPE4 had the most hydrophilic nature with an initial water in air contact angle value of 77.00 ± 1.28°, while CUPE12 was most hydrophobic, with a contact angle value of 98.91 ± 1.34°. Swelling studies indicated that the choice of monomer diol also affected the bulk properties of the CUPE family of polymers. CUPE4 and CUPE12 had the highest (168.50 ± 24.38%) and lowest (10.26 ± 2.83%) degrees of swelling in PBS, respectively, as depicted in Figure 6. The bulk swelling of the different family polymers decreased with increasing number of carbon atoms in the diol monomer used in the synthesis due to the hydrophobic nature of the larger methylene diol. Thus, one would expect that with a higher degree of crosslinking the CUPE polymers with lower number of methylene units would exhibit the lowest degree of swelling. However, the results demonstrate that the hydrophobicity of the diol plays a more predominant role than the crosslink density in determining water uptake and hence swelling, which is in agreement with published literature.[46]

This phenomenon was also evident in the accelerated degradation studies conducted on the different CUPE polymers in

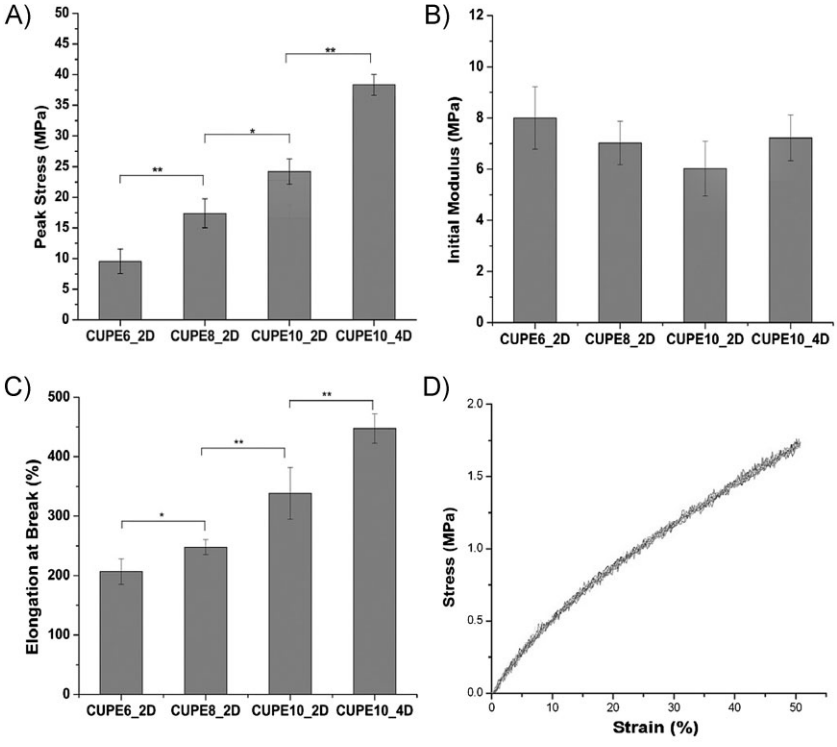

Figure 4. Mechanical properties of the different CUPE polymers. All the polymers shown were polymerized at 80 °C for 2 d except for CUPE10_4D which was polymerized for 4 d at 80 °C. Effect of diol component and post-polymerization conditions on the peak stress (A), initial modulus (B), break strain (C), and hysteresis (D) are shown. ** corresponds to $p < 0.01$ and * denotes $p < 0.05$. A minimum sample size of $N = 5$ was used for all tests.

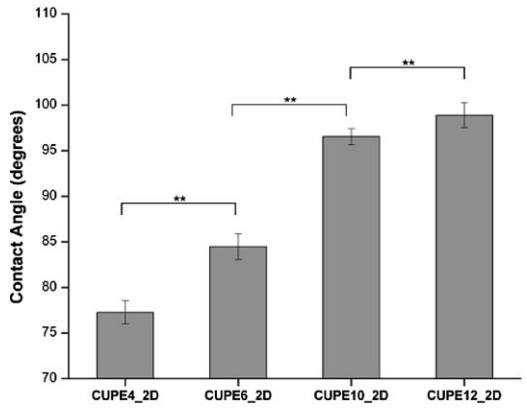

Figure 5. Initial contact angles of the different CUPE pre-polymers. Readings were taken for each specimen and averaged ($N = 8$). Contact angle was observed to increase by increasing the number of methylene units in the diol component. ** represents $p < 0.01$.

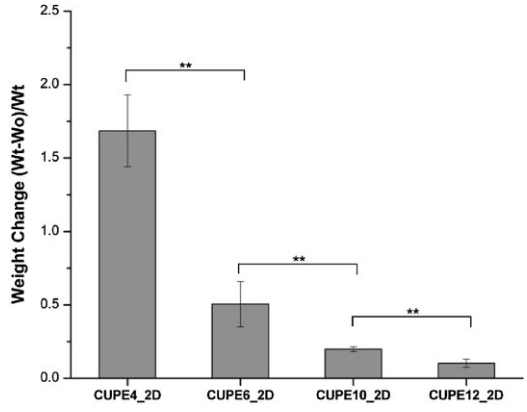

Figure 6. Bulk water uptake and swelling of the different CUPE pre-polymers. A minimum sample size of $N = 8$ was used for each polymer tested. Water uptake was found to increase with incorporation of more hydrophilic diols in polymer chain. ** denotes $p < 0.01$.

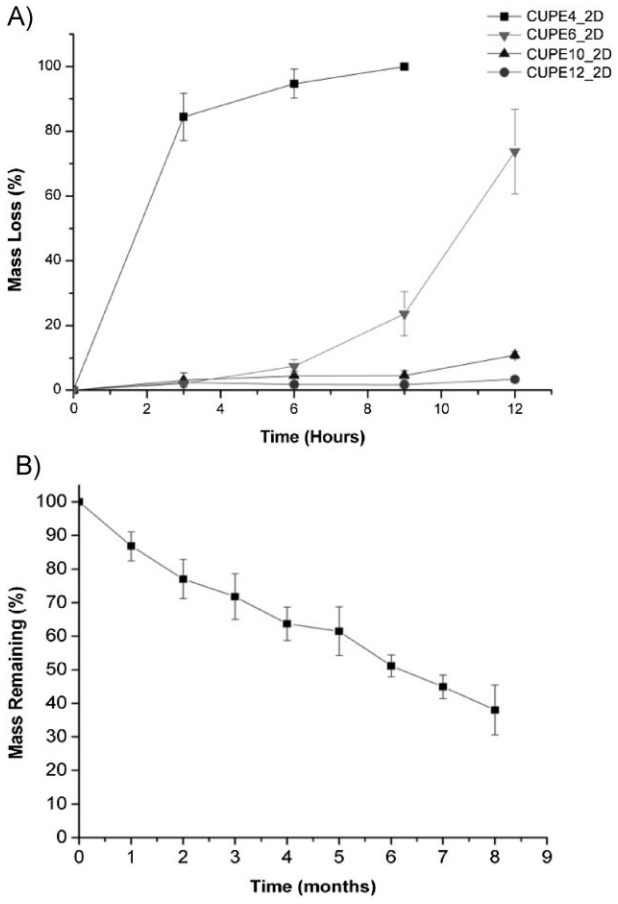

Figure 7. Degradation studies of different CUPE polymers in 0.05 M NaOH solution at room temperature. All the different polymers used in the PBS degradation study were polymerized at 80 °C for 2 d and different only in their diol component (A). Long-term degradation study of CUPE8 in PBS. The polymer was polymerized at 80 °C for 4 d prior to study. Sample size $N = 8$ (B).

0.05 M sodium hydroxide solutions. As seen from Figure 7A, it can be noted that the intrinsic nature of the polymers composed of more hydrophobic diols degraded slower than those containing more hydrophilic monomers. CUPE4 underwent complete degradation within 9 h, whereas, other polymers were still present at the final time point of 12 h. In contrast, CUPE12 demonstrated the slowest degradation profile, with 96.68 ± 0.97% of the polymer still remaining at the 12-h time point. The increased water uptake of the hydrophilic CUPE polymers would provide greater access to the hydrolytically labile ester bonds in the polymer backbone resulting in faster degradation through hydrolysis to yield to yield the original monomers, which can be metabolized and eliminated from the body. In addition to NaOH degradation, a long-term degradation study was also conducted on CUPE8 in PBS (Figure 7B). The results indicate that CUPE8 degraded steadily for 8 months, with only 37.99 ± 7.39% of the polymer remaining at the end of the last time point in the study. The initial biocompatibility of the different CUPE polymers was assessed by seeding NIH 3T3 fibroblasts and HASMCs on the polymer films and observing the morphology of the cells post-adhesion. Photomicrographs of the seeded films (Figure 8 and 9) indicate that both the cell types used were able to adhere to the CUPE polymers and express a normal phenotype with higher cell densities on CUPE polymers synthesized from longer length diols.[19,28] In our previous report,[28] we presented the foreign body response over a relatively short period of 1 and 4 weeks with CUPE8 scaffolds as the representative polymer. Figure 10 represents the foreign body response to CUPE8 scaffolds over a

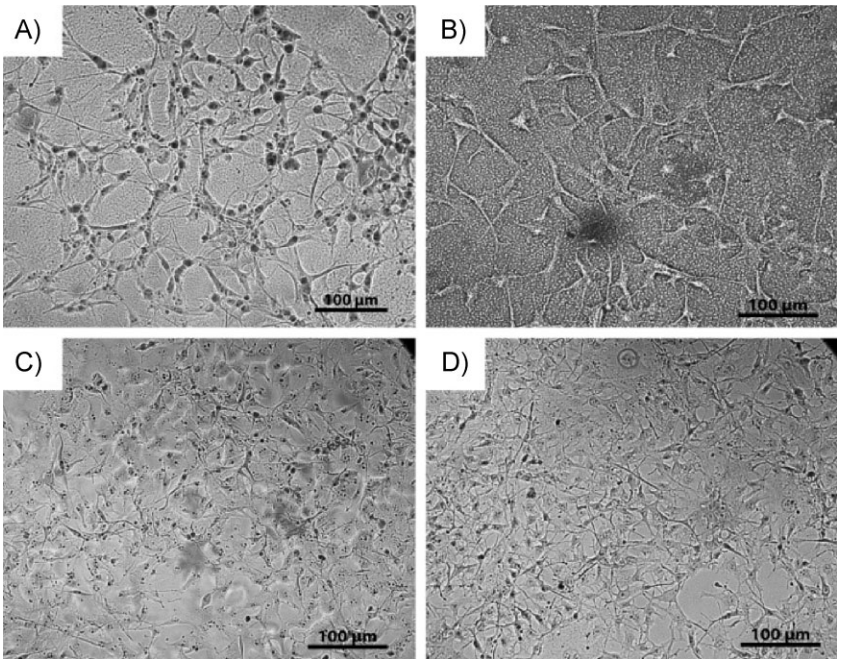

Figure 8. SEM images of NIH 3T3 fibroblasts growing on surface of CUPE films. Cells were allowed to grow and proliferate for 3 d post-seeding. Seeding density per film = 3×10^5 cells. Different films used include (A) CUPE4, (B) CUPE6, (C) CUPE10, and (D) CUPE12.

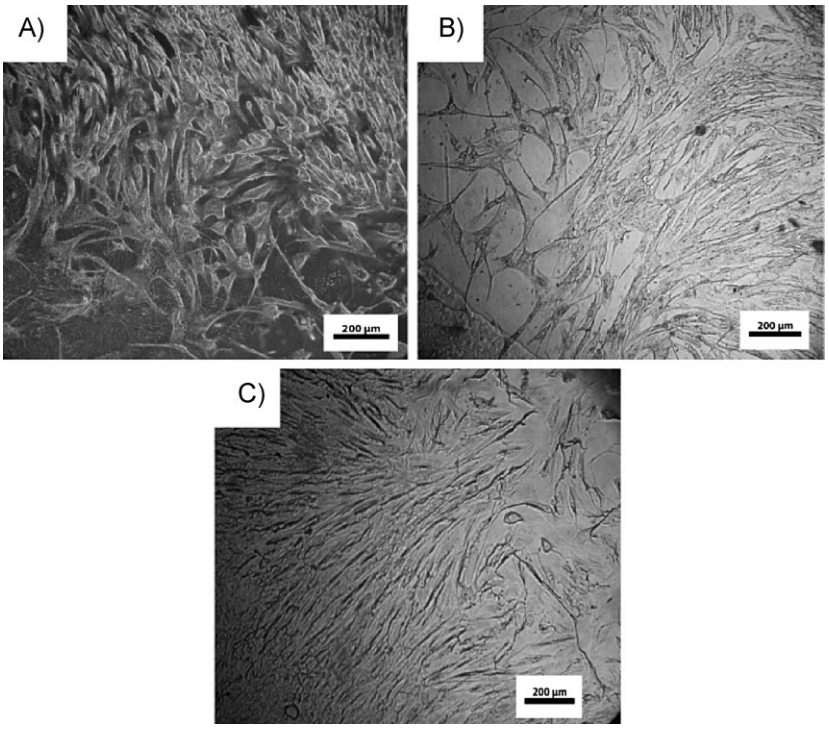

Figure 9. SEM images of HASMCs fibroblasts growing on surface of CUPE films. Cells were allowed to grow and proliferate for 3 d post-seeding. Seeding density per film = 3×10^5 cells. Different films used include (A) CUPE6, (B) CUPE10, and (C) CUPE12. CUPE4 was not used because of film dissolution over long culture time.

longer time period of 8 and 24 weeks with PLLA as the control. Although significant degradation could be observed in both at the later time period, CUPE and PLLA scaffolds were still present at 24 weeks. The absence of necrosis in and around the implants indicated a healthy healing response to both the materials. From Figure 10, it can be seen that even at 8 weeks 100% cellular infiltration was achieved in the CUPE and PLLA scaffolds. Both the scaffolds indicated the presence of a thin, non-uniform fibrous capsule. At 24 weeks, no tissue necrosis was observed in all test animals. The capsule could not be distinguished from the infiltrating cells. The scaffolds also lost their shape and showed reduced size compared to 8 weeks samples for both materials tested (Figure 10). These results indicate that, in addition to demonstrating better acute inflammatory responses than PLLA, CUPE also undergoes biodegradation in vivo and does not incite a significant long-term chronic inflammatory response. Although the gross inflammatory response was presented in this work, future studies will be focused on characterizing the specific cell types as part of the inflammatory response surrounding the implant.

Conclusion

A family of CUPE polymers with different diol components was synthesized and characterized. Varying the diol component was found to affect the different physical properties of the CUPE family members without significantly affecting the polymer performance with respect to cell/tissue compatibility. We have, therefore, established the diol component as an important parameter in controlling the structure/property relationship of the polymer in addition to diisocyanate concentration and post-polymerization conditions. This demonstrates the versatility with which the properties of CUPEs can be varied, thereby, rendering this polymer family attractive for a wide variety of tissue engineering applications.

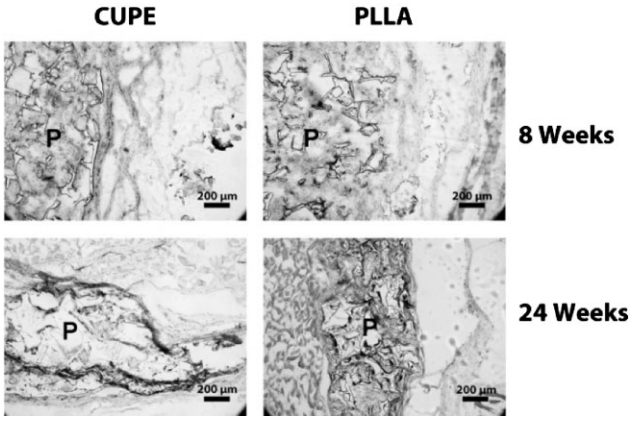

Figure 10. Host responses to CUPE and PLLA (control) implanted subcutaneously in SD rats. Histology analysis (H&E staining) for the long-term (8 and 24 weeks) implantation demonstrated that CUPE was degradable in vivo and did not elicit significant chronic inflammation. No tissue necrosis was observed in all test animals. *p*-Value indicates the polymer regions.

Acknowledgements: This work was supported in part by R21 award EB009795 from the National Institute of Biomedical Imaging and Bioengineering (NIBIB) (to J.Y.), a National Science Foundation (NSF) CAREER award 0954109 (to J.Y.), and a High Impact/High Risk grant RP110412 from Cancer Prevention & Research Institute of Texas (CPRIT). The authors also would like to thank Jinming Gao at University of Texas Southwestern Medical Center for his help on DSC measurements.

Received: February 19, 2011; Revised: May 2, 2011; Published online: DOI: 10.1002/mame.201100074

Keywords: biodegradable; biomaterials; elastomers; polyesters; structure/property relations

[1] L. M. Pineda, M. Busing, R. P. Meinig, S. Gogolewski, *J. Biomed. Mater. Res.* **1996**, *31*, 385.
[2] R. P. Meinig, B. Rahn, S. M. Perren, S. Gogolewski, *J. Orthop. Trauma* **1996**, *10*, 178.
[3] R. P. Meinig, C. M. Buesing, J. Helm, S. Gogolewski, *J. Orthop. Trauma* **1997**, *11*, 551.
[4] R. Zhang, P. X. Ma, *J. Biomed. Mater. Res.* **1999**, *45*, 285.
[5] R. Zhang, P. X. Ma, *J. Biomed. Mater. Res.* **1999**, *44*, 446.
[6] K. J. Burg, S. Porter, J. F. Kellam, *Biomaterials* **2000**, *21*, 2347.
[7] M. Borden, M. Attawia, C. T. Laurencin, *J. Biomed. Mater. Res.* **2002**, *61*, 421.
[8] J. Yang, Y. Zhang, S. Gautam, L. Liu, J. Dey, W. Chen, R. P. Mason, C. A. Serrano, K. A. Schug, L. Tang, *Proc. Natl. Acad. Sci. USA* **2009**, *106*, 10086.
[9] S. Yang, K. F. Leong, Z. Du, C. K. Chua, *Tissue Eng.* **2001**, *7*, 679.
[10] M. E. Lukashev, Z. Werb, *Trends Cell Biol.* **1998**, *8*, 437.
[11] D. E. Ingber, *FASEB J.* **2006**, *20*, 811.
[12] J. P. Stegemann, H. Hong, R. M. Nerem, *Appl. Physiol.* **2005**, *98*, 2321.
[13] J. P. Stegemann, R. M. Nerem, *Ann. Biomed. Eng.* **2003**, *31*, 391.
[14] D. MacKenna, S. R. Summerour, F. J. Villarreal, *Cardiovasc. Res.* **2000**, *46*, 257.
[15] J. J. Tomasek, G. Gabbiani, B. Hinz, C. Chaponnier, R. A. Brown, *Nat. Rev. Mol. Cell Biol.* **2002**, *3*, 349.
[16] J. Guan, M. S. Sacks, E. J. Beckman, W. R. Wagner, *J. Biomed. Mater. Res.* **2002**, *61*, 493.
[17] J. Guan, M. S. Sacks, E. J. Beckman, W. R. Wagner, *Biomaterials* **2004**, *25*, 85.
[18] Y. Wang, G. A. Ameer, B. J. Sheppard, R. Langer, *Nat. Biotechnol.* **2002**, *20*, 602.
[19] J. Yang, A. R. Webb, S. J. Pickerill, G. Hageman, G. A. Ameer, *Biomaterials* **2006**, *27*, 1889.
[20] J. Yang, A. R. Webb, G. A. Ameer, *Adv. Mater.* **2004**, *16*, 511.
[21] X. T. Li, J. Sun, S. Chen, G. Chen, *J. Biomed. Mater. Res.* **2008**, *87A*, 832.
[22] C. J. Bettinger, J. P. Bruggeman, J. T. Borenstein, R. S. Langer, *Biomaterials* **2008**, *29*, 2315.
[23] D. Gyawali, P. Nair, Y. Zhang, R. T. Tran, C. Zhang, M. Samchukov, M. Makarov, H. K. Kim, J. Yang, *Biomaterials* **2010**, *31*, 9092.
[24] R. T. Tran, P. Thevenot, D. Gyawali, J. C. Chiao, L. Tang, J. Yang, *Soft Matter* **2010**, *6*, 2449.
[25] R. T. Tran, P. Thevenot, Y. Zhang, L. Tang, J. Yang, *Materials* **2010**, *3*, 1375.
[26] D. Motlagh, J. Allen, R. Hoshi, J. Yang, K. Lui, G. A. Ameer, *J. Biomed. Mater. Res.* **2007**, *82A*, 907.
[27] J. Yang, D. Motlagh, A. R. Webb, G. A. Ameer, *Tissue Eng.* **2005**, *11*, 1876.
[28] J. Dey, H. Xu, J. Shen, P. Thevenot, S. R. Gondi, K. T. Nguyen, B. S. Sumerlin, L. Tang, J. Yang, *Biomaterials* **2008**, *29*, 4637.
[29] J. Dey, H. Xu, K. T. Nguyen, J. Yang, *J. Biomed. Mater. Res.* **2010**, *95A*, 361.
[30] S. E. Dahms, H. J. Piechota, R. Dahiya, T. F. Lue, E. A. Tanagho, *Br. J. Urol.* **1998**, *82*, 411.
[31] M. C. Lee, R. C. Haut, *J. Biomech.* **1992**, *25*, 925.
[32] J. A. Clark, J. C. Cheng, K. S. Leung, *Burns* **1996**, *22*, 443.
[33] R. Langer, J. P. Vacanti, *Science* **1993**, *260*, 920.
[34] S. A. Sell, M. P. Francis, K. Garg, M. J. McClure, D. G. Simpson, G. L. Bowlin, *Biomed. Mater.* **2008**, *3*, 11.
[35] X. Zong, H. Bien, C. Y. Chung, L. Yin, D. Fang, B. S. Hsiao, B. Chu, E. Entcheva, *Biomaterials* **2005**, *26*, 5330.
[36] C. C. Berry, G. Campbell, A. Spadiccino, M. Robertson, A. S. Curtis, *Biomaterials* **2004**, *25*, 5781.
[37] R. T. Tran, Y. Zhang, D. Gyawali, J. Yang, *Recent Patents Biomed. Eng.* **2009**, *2*, 216.
[38] R. Jayakumar, Y. S. Lee, S. Nanjundan, *J. Appl. Poly. Sci.* **2003**, *90*, 3488.
[39] J. Guan, W. R. Wagner, *Biomacromolecules* **2005**, *6*, 2833.
[40] F. Li, J. Hou, W. Zhu, X. Zhang, M. Xu, X. Luo, D. Ma, K. Kim, *J. Appl. Polym. Sci.* **1996**, *62*, 631.
[41] J. T. Garrett, J. Runt, *Macromolecules* **2000**, *33*, 6353.
[42] B. Chu, T. Gao, Y. Li, J. Wang, C. R. Desper, C. A. Byrne, *Macromolecules* **1992**, *25*, 5724.
[43] K. Nakamae, T. Nishino, S. Asaoka, *Sudaryanto, Int. J. Adhes. Adhes.* **1996**, *16*, 233.
[44] G. A. Skarja, K. A. Woodhouse, *J. Appl. Polym. Sci.* **2000**, *75*, 1522.
[45] K. Gorna, S. Gogolewski, *J. Biomed. Mater. Res.* **2002**, *60*, 592.
[46] D. S. Muggli, A. K. Burkoth, K. S. Anseth, *J. Biomed. Mater. Res.* **1999**, *46*, 271.
[47] S. Y. Lee, J. C. Lee, B. K. Kim, *Polym. Int.* **1997**, *42*, 67.